New Horizons in Earth Reinforcement – Otani, Miyata & Mukunoki (eds)
© 2008 Taylor & Francis Group, London, ISBN 978-0-415-45775-0

Validation of high seismic stability of a new type integral bridge consisting of geosynthetic-reinforced soil walls

H. Aizawa, M. Nojiri, D. Hirakawa, H. Nishikiori & F. Tatsuoka
Tokyo University of Science, Japan

M. Tateyama & K. Watanabe
Railway Technical Research Institute, Japan

ABSTRACT: Shaking table tests were performed on scaled models of four different bridge types: 1) the conventional-type, comprising of a pair of gravity-type abutments retaining unreinforced backfill; 2) the GRS RW bridge, comprising of a pair of geosynthetic-reinforced soil (GRS) retaining walls with full-height rigid (FHR) facings directly supporting a girder on the crest of the reinforced backfill; 3) the conventional integral bridge with unreinforced backfill, unifying a pair of FHR facings with a girder; and 4) a new type integral bridge comprising of a pair of GRS retaining walls having FHR facings (called the GRS integral bridge). It is shown that the seismic stability of the GRS integral bridge is highest among the four types examined because of several inherent structural advantages resulting in a monolithic behaviour of the whole bridge system.

1 INTRODUCTION

In many previous major earthquakes, including the 1995 Hyogoken Nambu and 2004 Niigata Chuetsu earthquakes, a number of conventional type bridges, typically those comprising of a pair of gravity-type abutments supporting a girder on the top and the unreinforced backfill on the back, totally collapsed and it took long time to be reconstructed. As a line structure, such as a railway and a highway, may lose its function for a long period even by collapse of a single bridge, the development of cost-effective bridge system, while having a high stability against level 2 design seismic load, has been required. In view of the above, we proposed a new type bridge system, called the GRS integral bridge (Fig. 1), combining the geosynthetic-reinforced soil (GRS) retaining wall (RW) technology and the conventional integral bridge system (with unreinforced backfill) (Nojiri et al., 2006; Aizawa et al., 2006; Hirakawa et al., 2006, 2007; Tatsuoka et al., 2007).

In this study, a series of model shaking table tests was performed to evaluate the seismic stability of the GRS integral bridge in comparison with those of the following three conventional bridge types:

1. *Gravity-type abutment bridge*: a pair of gravity-type abutment supports a girder on their top via movable and fixed supports while unreinforced backfill on their back.

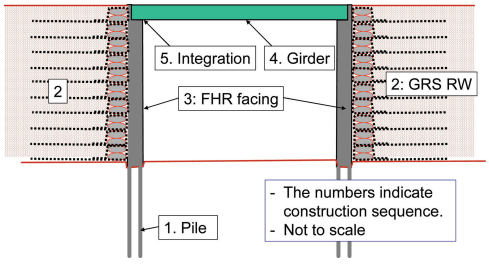

Figure 1. GRS integral bridge.

2. *GRS RW bridge*: a pair of geosynthetic-reinforced soil retaining walls (GRS RWs) with full-height rigid (FHR) facings directly support a girder via movable and fixed supports on sill beams placed on the reinforced backfill.
3. *Conventional integral bridge*: a girder is integrated with a pair of FHR facings while the backfill is unreinforced.

Tatsuoka et al. (2007) compare the structural features of the GRS integral bridge with those of these three conventional bridge types to highlight its advantages. Hirakawa et al. (2007) reports the effects of tensile resistance of reinforcement layers on the seismic stability on the GRS integral bridge.

2 TEST METHOD

2.1 *Apparatus*

A shaking table at Railway Technical Research Institute was used, which has a maximum excitation acceleration of about 1,500 gals with a maximum amplitude of horizontal displacement of ±5 cm when the load is 60 kN. The sand box, 205.8 cm-long ×60 cm-wide ×140 cm-high, was fixed on the shaking table. The front side wall of the box consists of a transparent tempered glass sheet, through which displacements and deformation of the model were observed. The other side wall consists of a steel plate with an inside face covered with a 0.2 mm-thick Teflon sheet to minimize side wall friction.

2.2 *Model subsoil and backfill and model bridges*

Fig. 2 presents the four bridge models. A 35 cm-high subsoil layer and 51 cm-high backfill were prepared by pluviating air-dried Toyoura sand throughout air using multiple sieves to a target initial relative density equal to 90%. Thin horizontal layers of black-dyed Toyoura sand particles were arranged in the subsoil layer and backfill to observe their deformation in the tests. The length similitude ratio of the bridge models was assumed to be 1/10. The model abutments and facings were made of basically duralumin. Their back face was made rough by gluing sandpaper #150. The model girder was made of steel having a mass of 25 kg and a length of 60.8 cm (i.e., the largest possible length to be accommodated in the sand box). By fixing a weight of 180 kg to the center of the girder, the equivalent girder length was made 6 m (i.e., 20 m in the prototype).

1. *Gravity-type abutment bridge (Fig. 2a):* A girder is supported by a pair of movable and fixed supports. The fixed support was allowed to rotate about a pin, while the movable support was allowed to horizontally slide along a linear rail.
2. *GRS RW bridge (Fig. 2b)*: A girder is supported in the same way as above. The bottom of the full-height rigid (FHR) facing was embedded 4 cm in the subsoil. The model reinforcement was a grid constituting of 0.2 mm-thick and 3 mm-wide phosphor bronze strips as the longitudinal members and 0.5 mm-diameter wire as the transversal members (Fig. 3). Sand particles were glued on their surface. Nine grid layers were placed at a vertical spacing of 5 cm in the backfill. Seven reinforcement layers were connected to the back of the FHR facings and two layers to the back of the sill beams.
3. *Integral bridge (Fig. 2c)*: A girder and FHR facings were connected to each other with a pair of L-shaped metal fixtures (20 cm-long, 5 cm-wide and 3 mm-thick). Fig. 4 shows the relationship between the moment, M, and the flexural angle, ϕ, from bending tests. It is likely that the initial low-stiffness

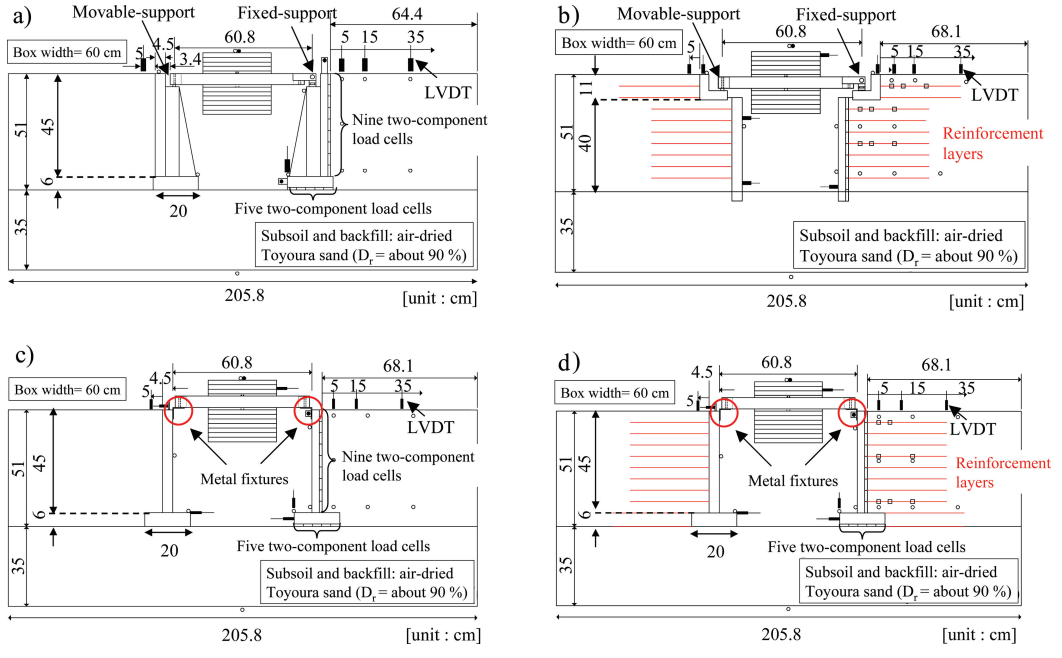

Figure 2. Four bridge models. a) gravity-type abutment bridge; b) GRS RW bridge; c) integral bridge with unreinforced backfill; and d) GRS integral bridge.

part of the measured M-ϕ relation is due to loose setting of the test specimen, so not reliable. It is assumed that the correct origin is located at point *a*. It was estimated that a flexural angle of about 0.9 degrees (from the point *a*) takes place by the weight of the bridge girder. So the metal fixture starts yielding at a flexural angle increment of about 2.6 degrees and exhibits the peak moment at an increment of 5.7 degrees. These are equivalent to shear strains (γ) in the backfill equal to about 4.5% and 9.9%. As the dense Toyoura sand exhibits the peak strength at $\gamma \sim 8$–12% (Tatsuoka et al., 1986), the fixtures have already started yielding and may start strain-softening when the backfill exhibits the passive failure. That is, the fixtures were designed not to become the major resisting structural component when the collapse of the bridge becomes imminent. It was considered that it is the case with proto-types.

4. *GRS integral bridge (Fig. 2d)*: A girder and a pair of FHR facings were integrated in the same way as the integral bridge model described above. In total ten reinforcement layers were arranged in the backfill, eight layers connected to the back of the facing at a vertical spacing of 5 cm and two layers to the back of the facing foundation at the vertical spacing of 6 cm. As the connection strength was sufficiently large, eventually pull-out failure took place as described by Hirakawa et al. (2007).

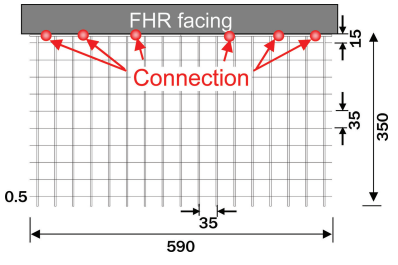

Figure 3. Model grid reinforcement.

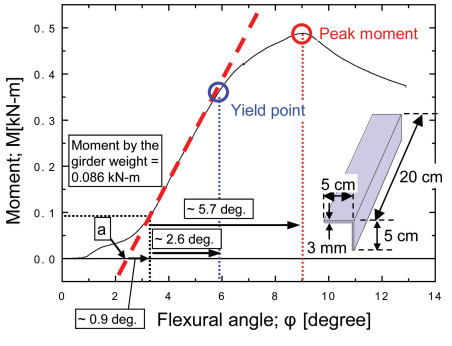

Figure 4. Relationship between moment and flexure angle of L-shaped metal fixture.

2.3 *Loading conditions*

A surcharge of 1 kPa was placed on the crest of the backfill simulating the railway conditions. The models were subjected to horizontal sinusoidal acceleration consisting of 20 waves at a frequency of 5 Hz at each loading stage. The input acceleration was increased incrementally at a step of 100 gals from 100 gals until the respective models ultimately collapsed.

3 TEST RESULTS

3.1 *Cumulative residual displacements*

Fig. 5a shows the cumulative residual rotational angle of the facing (θ) plotted against the amplitude of base acceleration (α_b). With the gravity-type abutment and GRS RW bridges, the displacements of the facing on the side supporting the girder via a fixed support is presented in Fig. 5a (and also in Fig. 5b). With the GRS RW bridge, the rotational angle of the sill beam is also presented. The angle θ is positive when the top of the facing overturns outward relative to the bottom (i.e., the active direction). Fig. 5b presents the cumulative residual outward lateral displacements (d_b) at the bottom of abutment or facing against α_b. With the GRS RW bridge, the displacements at the sill-beam are also presented. Figs. 6a and 6b present the cumulative residual settlements of the backfill at distances of 5 cm and 35 cm back of the abutment or facing on the side supporting the girder by a fixed support. The following trends of behaviour may be seen:

1. *Gravity-type abutment bridge*: When α_b became 180 gals, by large inertia of the girder at its top via a fixed-support, the abutment started overturning outward at the top and sliding outward at the bottom. At the same time, the backfill started settling at a distance of 5 cm back of the facing. The settlement at a distance of 35 cm was not noticeable until the end of the test. When α_b became 255 gals, the over-turning at the top and sliding at the bottom became significant and a general shear band was formed in the backfill (Fig. 7). No double, this type of bridge was weakest among the four bridge types.
2. *GRS RW bridge*: When α_b becomes 383 gals, the sill beam started largely overturning in the active direction associated with failure in the backfill immediately below the toe of the sill beam due to large moment caused by the inertia of the girder. On the other hand, the settlement in the backfill back of the sill beam still remained very small (Fig. 6b), showing that the GRS RW itself was still stable. As α_b increased to 472 gals, the rotation and outward lateral displacement of the sill beam became much larger, while the settlement increased and a shear band was formed in the backfill back of the sill

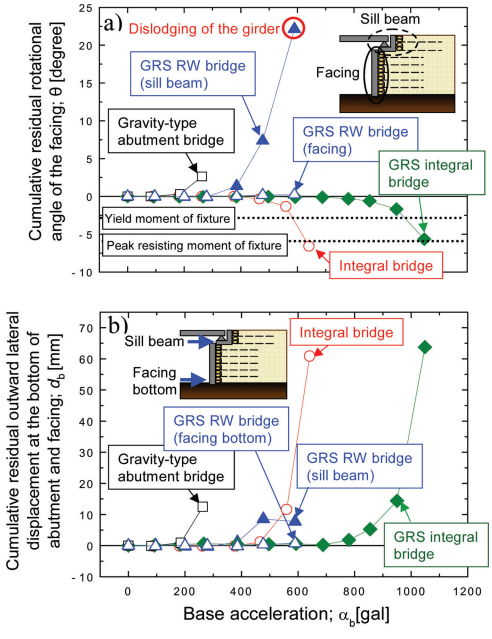

Figure 5. Relationships between a) facing rotation angle and b) outward displacement at the facing bottom and base acceleration.

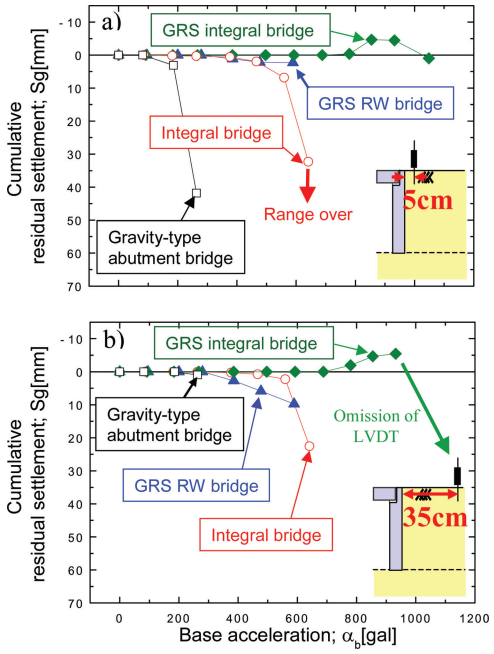

Figure 6. Relationships between cumulative residual settlement of the back-fill at positions of a) 5 cm and b) 35 cm from the top of wall and base acceleration.

beam (denoted as 1 in Fig. 8). At $\alpha_b = 589$ gals, the girder contacted and pushed inward the other sill beam having a movable support, which triggered the formation of a general shear band in the backfill (2 in Fig. 8). The mass of the sill beam was too small to resist against the large inertia of the girder, while the tensile reinforcement layers attached at the back of the sill beam did not resist against this force. On the other hand, the deformation of the GRS walls remained still small (Fig. 5). It is clear that a low seismic stability of this type of bridge is due to a very low of dynamic stability of the sill beams.

3. *Integral bridge*: When α_b became 560 gals, the L-shaped metal fixtures, connecting the facings and girder, started yielding and the facings started noticeably rotating forward about the top, as the girder functioned as a strut against the earth pressure activated on the facings. The backfill started settling noticeably, while shear bands were formed in the backfill on the right (1 in Fig. 9). At $\alpha_b = 641$ gals, the facings started rotating significantly forward, and circular shear bands were formed (2 in Fig. 9), and the backfill settled down at distances of not only 5 cm but also 35 cm in back of the facing.
4. *GRS integral bridge*: It was only when α_b became as high as 799 gals that the facings started rotating noticeably like the integral bridge, as described

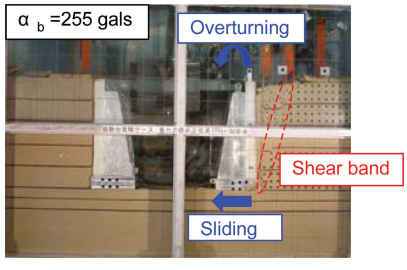

Figure 7. Gravity type abutment bridge after shaking at $\alpha_b = 255$ gals.

above. The backfill heaved slightly by passive movements at the top of the facing by the inertia of the girder. As α_b increased to 950 gals, the rotation of the facing increased but much more gradually than the other types of bridge. Shear bands were formed in the unreinforced backfill zone immediately back of the reinforced zones (Fig. 10). When α_b became 1,048 gals, the L-shaped metal fixtures yielded significantly and the bottom of the facings was largely pushed out associated with large rotational movements of the facing and reinforced backfill zone about the top of the facing. This failure mode can also be seen from significant settlement (about 2 cm by the photogrametric method)

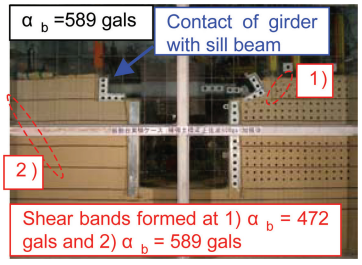

Figure 8. GRS RW bridge after shaking at $\alpha_b = 589$ gals.

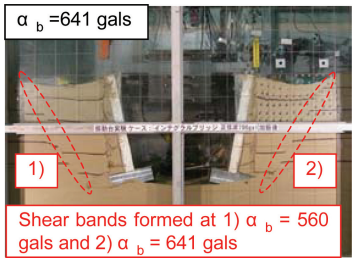

Figure 9. Integral bridge after shaking at $\alpha_b = 641$ gals.

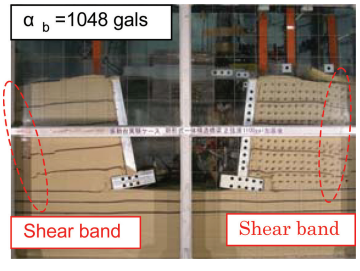

Figure 10. GRS integral bridge after shaking $\alpha_b = 1048$ gals.

of the backfill at a distance of 35 cm from the back of the facing, compared with small settlement at a distance of 5 cm (Fig. 10). This monolithic behaviour of the facing and backfill is due to firm connections between the full-height rigid facing and the reinforcement layers arranged in the backfill, which greatly improved the seismic stability of the integral bridge.

3.2 *Dynamic responses*

Fig. 11 shows the time histories of base acceleration at the shaking table, response acceleration at the girder and sill beam, average lateral earth pressure, p, on the back of the abutment supporting the girder via a fixed-support or the facing of integral bridge and average normal pressure, σ, at the bottom of the abutment or the facing footing. The earth pressure, p and σ, were obtained by averaging the loads measured with respective sets of local load cells (Fig. 2). With the GRS RW bridge, the horizontal acceleration at the sill beam supporting the girder via a fixed-support is presented instead of σ in the other cases. Acceleration is defined positive when the displacement of the facing on the side with the fixed girder-support is at the passive state (i.e., when the inertia of the girder acting to this facing is in the passive direction).

1. *Gravity type abutment bridge (Fig. 11a)*: During shaking at $\alpha_b = 255$ gals, the σ value at the abutment bottom became the minimum when the abutment top was at the passive state, which it was not very small initially. As α_b increased, the response of the girder increased associated with the bearing capacity failure in the subsoil below the abutment base, which resulted in a substantial decrease in the minimum of σ. Subsequently, the abutment base started moving toward the active direction while the abutment top was moving toward the passive direction. As a result, the minimum of σ started increasing associated with a decrease in the passive earth pressure of p.
2. *GRS RW bridge (Fig. 11b)*: The earth pressure, p, was much smaller than those with the other bridge types, because the facing and reinforced backfill behaved like a monolith in a rather stable manner. On the other hand, as α_b increased, the ratios of the response acceleration of the bridge girder (α_g) and sill beam (α_{sb}) to the base acceleration (α_b) became larger. During shaking at $\alpha_b = 589$ gals, both α_g and α_{sb} increased suddenly, which was due to sudden unstable over-turning of the sill beam supporting the girder via a fixed-support.
3. *Integral bridge (Fig. 11c)*: When α_b was 378 gals, both of pressures, p and σ, exhibited steady values. During shaking at $\alpha_b = 470$ gals, the response acceleration of the girder (α_g) was increasing at a noticeable rate, associated with a large increase in the displacements at the top of the facings. The σ value at the footing base became the maximum when the facing top was at the active state and the minimum when the facing top was at the passive state. The both decreased at a large rate with time, which was due to an increase in unstable large rotation of the facing: i.e., when the facing top was at the passive state, the toe area of the footing base separated from the subsoil while the subsoil below the heel area collapsed. A similar phenomenon took place when the facing top was at the active state.
4. *GRS integral bridge (Fig. 11d)*: At $\alpha_b = 799$ gals, the bridge was still rather stable, the girder and the facings together with the reinforced backfill behaving as an integrated structure. When α_b became 860 gals, both the maximum and minimum of σ on the facing footing base started decreasing by

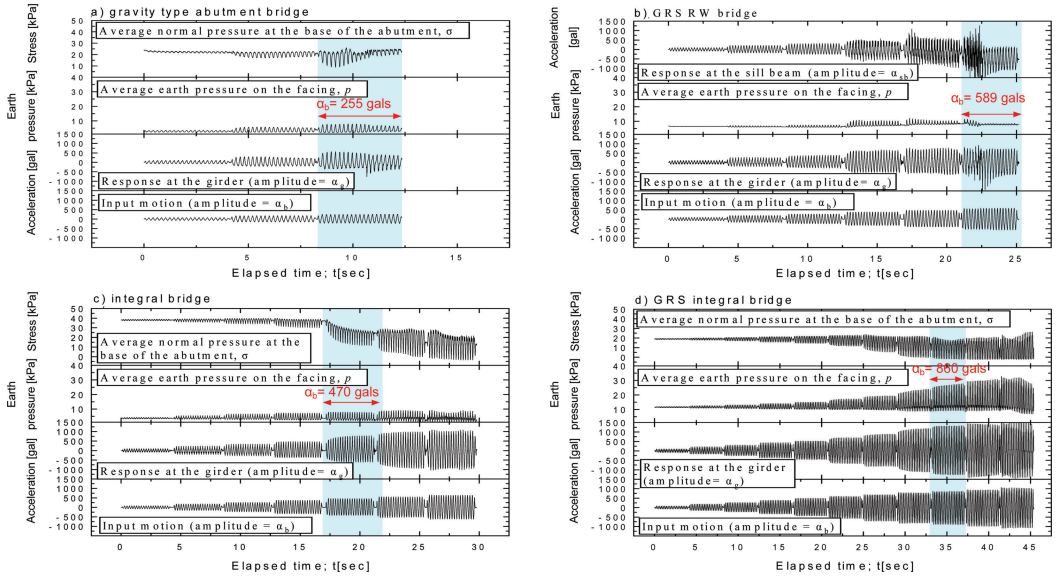

Figure 11. Time histories of measured physical quantities: a) gravity type abutment bridge; b) GRS RW bridge; c) integral bridge; and d) GRS integral bridge.

the mechanisms explained above with the integral bridge. When α_b became 1,048 gals, the response at the girder, α_g, increased significantly whereas the earth pressures, p, on the back of the facing started decreased. This was due to the monolithic rotational displacements about the facing top of the facing and reinforced backfill that became significant. The maximum of the earth pressure, p, with the GRS integral bridge was generally much larger than with the other types. This trend of behavior means that large tensile force was activated in the reinforcement, showing that the reinforcement contributed effectively to the stabilization of the bridge. This large increase in the earth pressure does not damage the facing, as the facing is a continuous rigid beam having many supports (i.e., the reinforcement layers) with a short span.

3.3 *Failure mode of GRS integral bridge*

Fig. 12 shows the distributions with depth of the earth pressure at 10*th* cycle at the respective shaking stages on the back of the facing of the GRS integral bridge when the top of the facing was at the largest passive and active displacements. Fig. 13 shows the relationships between the maximum tensile force in the reinforcement at selected points immediately back of the facing. The following trends of behaviour may be seen from Figs. 12 and 13:

1. When the facing top was at the passive state, the earth pressure was large (i.e., passive earth pressure) in the upper part of backfill while it was small (i.e., active earth pressure) in the bottom part of backfill. The trend was opposite when the facing top was at the active stage. Relatively low passive earth pressure near the facing bottom was due to the friction between the backfill and the subsoil. These trends of earth pressure are due to rotational displacements of the facing relative to the backfill.
2. The rotation displacements of the facing was resisted effectively only by the lower reinforcement layers (Fig. 13).
3. The passive earth pressure in the upper part of the backfill (Fig. 12a) was largest when $\alpha_b = 799$ gals and decreased as α_b increased subsequently. This means that the backfill exhibited passive failure, which resulted in an increase in the rotation of the facing relative to the backfill. Then, the displacement therefore the inertia of the girder increased and the center of the facing rotation relative to the backfill was shifted download, which all accelerated the passive yielding of the backfill, increasing the facing rotation associated with sliding at the facing foundation, and increased the tensile force in the reinforcement. Then, excessive tensile force in the lower reinforcement layers resulted in the connection failure or/and pull-out failure of the reinforcement.

These results indicate that the use of a sufficient number of tensile reinforcement layers having sufficiently high rupture strength, connection strength and

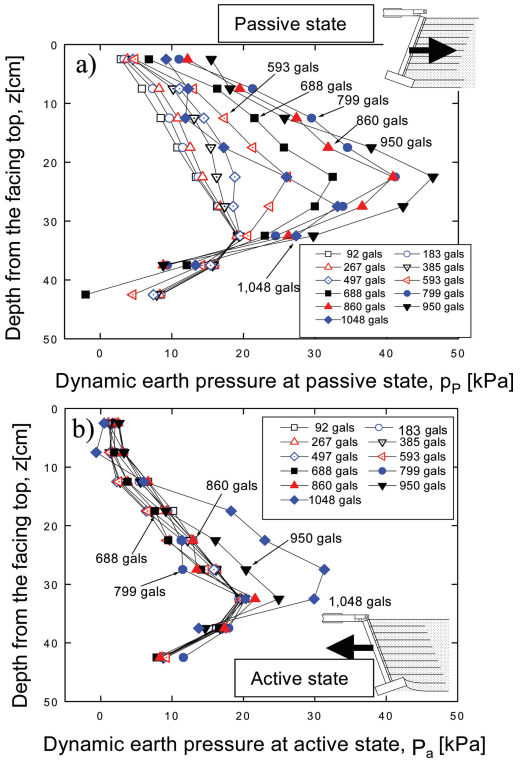

Figure 12. Earth pressure distribution with depth on the facing at 10th cycle at each stage, GRS integral bridge.

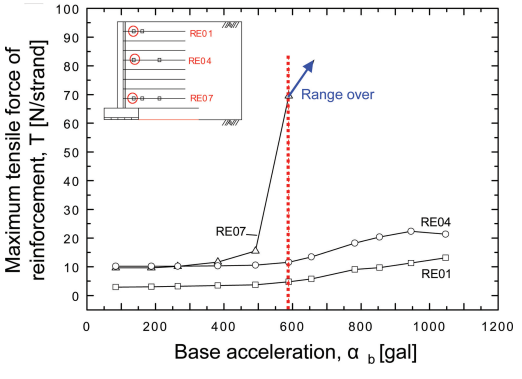

Figure 13. Relationship between tensile force of rein-forcement and base acceleration, GRS integral bridge.

pull-out strength, in particular at the lower part of the facing, is essential for a high seismic stability of GRS integral bridge.

4 CONCLUSIONS

The following conclusions can be obtained from the results from 1-g shaking table tests on four different bridge models presented in this paper:

1. The GRS integral bridge has the highest seismic stability among the different bridge types examined in the present study.
2. The collapse of the GRS integral bridge was associated with the rotation of the facing relative to the backfill with the bottom end being pushed out. The use of a sufficient number of reinforcement layers having a sufficient tensile resistance is essential for a high seismic stability of GRS integral bridge.

REFERENCES

Tatsuoka et al., (2007): A new type integral bridge consisting of geosynthetic-reinforced soil walls, *Proc. of IS Kyushu*, 2007 (this volume)

Hirakawa et al., (2007): Effects of the tensile resistance of reinforcement embedded in the backfill on the seismic stability of GRS integral bridge, *Proc. of IS Kyushu*, 2007 (this volume)

Aizawa et al., (2006): Comparison of cost-performance effectiveness of conventional and new types of bridge systems consisting of unreiforced or reinforced soil, *Geosynthetics Engineering Journal, IGS Japanese Chapter*, Vol. 21, pp. 175–182 (in japanese)

Nojiri et al., (2006): Evaluation of dynamic failure modes of various bridge types by shaking table tests, *Geosynthetics Engineering Journal, IGS Japanese Chapter*, Vol. 21, pp. 159–166.

Tatsuoka et al., (1986): Strength and deformation characteristics of sand in plane strain compression at extremely low pressures, *Soil and Foundations*, Vol. 26, No. 1, pp. 65 ~ 84, 1986